Ecological Modelling 498 (2024) 110883

Contents lists available at ScienceDirect

Ecological Modelling

journal homepage: www.elsevier.com/locate/ecolmodel

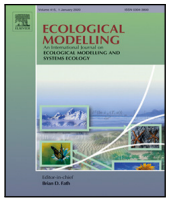

Exploring aquaculture related traits of the grooved carpet shell (*Ruditapes decussatus*) in relation to other bivalve species using Dynamic Energy Budget theory

Merel Lanjouw [a,*], Henrice M. Jansen [a], Jaap van der Meer [a,b]

[a] Aquaculture and Fisheries Group, Wageningen University & Research, De Elst 1, Wageningen, 6708 WD, The Netherlands
[b] Wageningen Marine Research, Wageningen University & Research, Korringaweg 7, Yerseke, 4401 NT, The Netherlands

ARTICLE INFO

Dataset link: Add-my-Pet website

Keywords:
Dynamic Energy Budget theory
Ruditapes decussatus
Grooved carpet shell
Aquaculture
Production efficiency
Bivalves

ABSTRACT

To assess the potential of the grooved carpet shell (*Ruditapes decussatus*) for aquaculture in Europe, we used Dynamic Energy Budget (DEB) theory to perform extensive parametrization on the species and compared its energy allocation strategy with those of commonly farmed bivalve species: mussels (*Mytilus edulis* and *Mytilus galloprovincialis*), oysters (*Ostrea edulis* and *Magallana gigas*), the common cockle (*Cerastoderma edule*), and great scallop (*Pecten maximus*). The comparison was based on DEB primary parameters relevant to aquaculture production, such as maximum assimilation rate and kappa, which represents the fraction of energy allocated to maintenance and growth, and compound parameters like the von Bertalanffy growth coefficient and maximum storage density. Furthermore, we evaluated the production efficiency at the population level, which represents the ratio of assimilated energy converted into biomass. Our results revealed notable differences in energy utilization strategies among species. However, uncertainties in parameter estimation and environmental factors challenge the direct translation of these parameters to real-world aquaculture, therefore our interpretation focuses on how these parameters might influence a species' potential for aquaculture. The grooved carpet shell exhibits a balanced energy allocation strategy with a low growth coefficient and low maintenance costs, leading to high production efficiency. Similarly, the common mussel focuses on growth with significant biomass investment over reproduction, while the Pacific oyster and Mediterranean mussel prioritize reproductive development. The flat oyster and scallop demonstrate rapid growth at the cost of the low production efficiencies. The grooved carpet shell and mussels face constraints such as limited reserves, making them comparatively more susceptible to low food quality and quantity. In contrast, high storage densities in species like the common cockle, scallop, and Pacific oyster suggest resilience to fluctuating food conditions. These findings, along with both agreements and discrepancies with existing literature, highlight the need for further experimental research to refine DEB parameters and enhance their application in aquaculture. Overall, the DEB framework proves effective for exploring aquaculture traits across species and underscores the need for additional work on temperature-related processes, life-history events, and morphological variation.

1. Introduction

The rise of the global population and need for food safety has led to an increasing interest in low-trophic aquaculture (Campbell et al., 2017; Chary et al., 2023; van der Meer, 2020). Bivalves are a promising avenue, with high nutritional values and low environmental impacts compared to higher trophic marine species or terrestrial livestock (Koehn et al., 2022; van Riel et al., 2023). In order to predict productivity and ecosystem impacts, also known as production and ecological carrying capacity (Inglis et al., 2002), we need to gain deeper understanding of the physiology of a range of aquacultural species in relation to their environment. Using one unified theory to research these individual dynamics allows a comparison among species. Subsequently, the resulting insights can be used in ecosystem modelling to predict productivity on different locations, scales, and environments (van der Meer et al., 2022). Dynamic Energy Budget (DEB) theory provides a comprehensive framework applicable to all organisms, facilitating both intra- and inter-specific comparisons (Cardoso et al., 2006). Its increasing use in ecological modelling can be attributed to its broad applicability and the need to understand individual dynamics in relation to the environment. DEB-based models use various primary

* Corresponding author.
E-mail address: merel.lanjouw@wur.nl (M. Lanjouw).

https://doi.org/10.1016/j.ecolmodel.2024.110883
Received 16 April 2024; Received in revised form 6 September 2024; Accepted 13 September 2024
Available online 26 September 2024
0304-3800/© 2024 The Author(s). Published by Elsevier B.V. This is an open access article under the CC BY license (http://creativecommons.org/licenses/by/4.0/).

parameters to describe energy flows in and through organisms, looking at assimilation, growth, maintenance, maturation, and reproduction, in relation to temperature and food availability (Kooijman, 2000). These primary DEB parameters (or compound parameters, which are combinations of primary parameters) can be used to compare different strategies among species, where certain parameters provide insight into how resources are assimilated and allocated by the organism, as well as the efficiency at which the resource is utilized for internal processes. Furthermore, DEB parameters can be used to calculate species-specific traits, reflecting the organisms' life history events, resource usage, mortality and growth rates at the individual or population level. For instance, the von Bertalanffy growth coefficient $\dot{r}_B$, which is a compound parameter, is an individual trait that helps predict how quickly an organism can reach commercial size, while the maximum storage density $[E_m]$, which is also a compound parameter, reflects its capacity to endure periods of low food availability. The maximum assimilation rate $\{\dot{p}_{Am}\}$ is the (primary) parameter giving the rate for utilizing available food resources and the fraction of energy allocated to growth (primary parameter κ) reveals the strategy for balancing growth and reproduction. The yields of structure and reserves on food (which are derived properties or traits) reveal how efficiently assimilated energy is converted into biomass at the population level. By comparing these parameters and traits, we can better understand the energy utilization strategies of various bivalve species and their potential performance in aquaculture settings. DEB model parametrizations have been performed on many aquatic species, including those commonly used in aquaculture, resulting in a substantial database. In Europe, bivalve aquaculture currently consists mainly of blue mussels (*Mytilus edulis* and *Mytilus galloprovincialis*), the native flat oyster (*Ostrea edulis*), invasive Pacific oyster (*Magallana gigas*) and great scallop (*Pecten maximus*) (Jansen et al., 2016; Wijsman et al., 2019), and all these species have been parametrized in DEB and analysed by various studies: blue mussel by Rosland et al. (2009), Sarà et al. (2012) and Taylor et al. (2021), flat and Pacific oyster by Stechele et al. (2022), and great scallop by Lavaud et al. (2014). Additionally, the common cockle, (*Cerastoderma edule*), having been significant export product of fisheries in the Netherlands (Pronker et al., 2015), shows promise for aquaculture, and has been parameterized by Cardoso et al. (2006). Yet, many native and edible species in Europe with cultivation potential have not yet undergone comprehensive DEB parameterization, which is essential for their inclusion in comparative analyses and consequent modelling efforts. The grooved carpet shell (*Ruditapes decussatus*) is one of these species. While Lopes (2017) initiated the DEB parameterization for this species, their work was based on limited data and was not thoroughly analysed in a dedicated publication. Consequently, accurately estimating all parameters and understanding the environmental effects on this species requires further efforts. The grooved carpet shell, *Ruditapes decussatus* (Linnaeus, 1758), is a clam found along the coast of Western Europe, ranging from the North Sea and North-Eastern Atlantic Ocean to the Mediterranean Sea. The clam represents an important source of income in many regions, especially in Portugal where the clam constitutes 27% of the total aquaculture revenue (Machado et al., 2018), but also in Turkey (Serdar and Lök, 2009), France (FAO, 2006), Egypt (Mohammad et al., 2014), and Spain (Rodríguez-Moscoso and Arnaiz, 1998). Although not currently cultivated north of France, its natural occurrence, long shelf life, and international market value suggest potential for production in more northern regions (FAO, 2006). The aim of this study is to apply DEB theory to gain insight into the characteristics of the grooved carpet shell as an aquacultural species, to understand its response to different environmental conditions, and to perform a comparative analysis of individual and population traits of the clam with other bivalve species viable for aquaculture in European temperate waters. The aim will be achieved through three steps: (1) estimation of species-specific parameters for the grooved carpet shell using datasets from various locations and experimental setups, (2) calculating the individual and population traits for the grooved carpet shell, (3) comparison of growth and reserve related parameters, individual and population traits with those of other bivalve aquaculture species.

2. Method: Parameter estimation

2.1. Adjustments to the standard DEB model

A model based on dynamic energy budget (DEB) theory was used here to estimate and assess the parameters and traits dictating growth, maturation and reproduction in the grooved carpet shell. For a comprehensive explanation of DEB theory and its assumptions, we refer to Kooijman (2010) and van der Meer (2006).

The life cycle of the grooved carpet shell consists of a larval and settlement phase, and therefore we adopted the typified abj DEB model, which is commonly used for bivalve species. The abj-model differs from the standard DEB model in its addition of a larval stage, between birth and puberty, to the standard three phases: embryonic, juvenile and adult. According to DEB theory we define birth as the moment organisms starts feeding, which occurs after about one to two days after fertilization for the grooved carpet shell, when the digestive tract forms and the cilia evolve into the velum (organ used swim and feed), marking the veliger stage (Aranda-Burgos et al., 2014). The larval stage ends when the clam enters metamorphosis after approximately twenty-seven days. During metamorphosis the larvae settle and lose the velum, but develop the mature shell, reproductive organs and gills. Sexual maturity, defined as puberty in DEB, is typically attained after one to two years, initiating the reproductive phase (Mohammad et al., 2014; Pérez-Camacho, 1980).

The standard model assumes species are isomorphic, meaning that they do not change in shape over time. However, the addition of the larval stage is accompanied by a change in shape of the organism and an acceleration of growth between birth and metamorphosis. This metabolic acceleration is modelled as V1-morphy, where surface area remains proportional to volume until the maturity threshold for metamorphosis, E_H^j (J), is reached and the clam continues development according to the standard DEB model. We added three additional parameters to the standard DEB model, first the maturity at metamorphosis, E_H^j, and consequently two additional shape coefficients, δ_M, for the egg and larval stage. Lastly, an acceleration factor s_M was added to ensure continuity after acceleration. Data on the age and size of these life-history events were used to estimate the maturity thresholds at birth E_H^b, metamorphosis E_H^j and puberty E_H^p.

In addition to estimating the abj-model parameters, functional responses (f) were estimated for some datasets, which is necessary when data on food conditions are unavailable (Cardoso et al., 2006; Lavaud et al., 2019).

2.2. Optimization procedure

The Add-my-Pet portal (AmP) contains MATLAB (The MathWorks Inc., 2023) scripts for estimating DEB model parameters for various animal species. We used the existing entry for the grooved carpet shell developed by Lopes (2017) as a basis for estimation using the existing four files: the mydata file with zero- and uni-variate observational data, the predict file for model predictions, the parsinit file with initial parameters, and the run file for setting optimization conditions. Additionally, the DEBtool software package was used for the estimation procedure (Marques et al., 2018). The DEBtool offers two estimation procedures, we used the Nelder–Mead simplex method for the parameter estimation, which minimizes the weighted sum of squared deviations between predictions and data, yielding mean relative errors and symmetric mean squared errors (Lika et al., 2011). DEBtool also allows users to assign weights to different data types, prioritizing more reliable data. More accurate data received higher weights, while datasets with many outliers were weighted less to prevent skewed predictions. Zero-variate data, such as egg size and size at birth, received higher weights due to lower variability compared to trend data or life history events such as puberty.

Table 1
DEB parameter values for the grooved carpet shell at reference temperature of 20 °C. The reference temperature and searching rate were based on reference values by Lika et al. (2011).

Notation	Units	Value	Description
T_{ref}	K	293.1	Reference temperature
T_A	K	3459	Arrhenius temperature
z	–	1.025	Zoom factor
$\{\dot{F}_m\}$	L d^{-1} cm^{-2}	65	Maximum specific searching rate
κ_{X1}	–	0.6859	Digestion efficiency of food to reserve for *I. galbana* diet
κ_{X2}	–	0.472	Digestion efficiency of food to reserve for *T. suecica* diet
κ_{X3}	–	0.5497	Digestion efficiency of food to reserve for *P. tricornutum* diet
$\dot{v}$	cm d^{-1}	0.03201	Energy conductance
κ	–	0.8055	Allocation fraction to soma
κ_R	–	1	Reproduction efficiency
$[\dot{p}_M]$	J d^{-1} cm^{-3}	5.484	Volume specific somatic maintenance
$\dot{k}_J$	d^{-1}	0.002	Maturity maintenance rate coefficient
$[E_G]$	J cm^{-3}	2346	Specific cost for structure
E_H^b	J	0.0006386	Maturity at birth
E_H^j	J	0.03763	Maturity at metamorphosis
E_H^p	J	1119	Maturity at puberty
$\ddot{h}_a$	d^{-2}	5.483 × 10^{-9}	Weibull aging acceleration
s_G	–	0.0001415	Gompertz stress coefficient
δ_{M1}	–	1.192	Shape coefficient before metamorphosis
δ_{M2}	–	0.5864	Shape coefficient after metamorphosis
δ_{MY}	–	1.744	Shape coefficient egg
$\{\dot{p}_{Am}\}$	–	6.9807	Maximum surface specific assimilation rate

Table 2
Zero-variate data, a point-specific value describing the individual at a specific moment in their life-history, and predicted value from the DEB model of the grooved carpet shell. T: temperature and RE: relative error.

Description	DEB notation	T	Data	Prediction	Units	RE
Age at birth[a]	a_b	20 °C	1.625	1.74	d	0.07
Age at metamorphosis[a]	a_j	20 °C	27	20.95	d	0.22
Age at metamorphosis[b]	a_j	28 °C	13	15.32	d	0.18
Time since birth at puberty[c]	a_p	20 °C	365	521	d	0.43
Life span[d]	a_∞	20 °C	2920	2919	d	<0.01
Egg diameter[a]	L_0	–	0.0067	0.0069	cm	0.02
Length at birth[a]	L_b	–	0.01	0.0087	cm	0.13
Length at metamorphosis[a]	L_j	–	0.0208	0.0340	cm	0.64
Length at puberty[c]	L_p	–	2	2.11	cm	0.06
Ultimate total length[c]	L_∞	–	6.8	6.8	cm	<0.01
Daily egg production[e]	$\dot{R}_\infty$	17 °C	2.20 × 10^4	2.05 × 10^4	# d^{-1}	0.07

[a] Aranda-Burgos et al. (2014).
[b] Beiras et al. (1994).
[c] Pérez-Camacho (1980).
[d] Urrutia et al. (1999).
[e] Maynou et al. (2020).

In order to ensure parameters remained within realistic ranges, we implemented filters in the estimation procedure, constraining the functional response and digestion efficiency between 0 and 1, and assessed the realism of output parameters by comparing them to other bivalve entries. We also re-ran the estimation procedure with different combinations of starting values. Some parameters, like searching rate and reference temperature and were based on reference values from Lika et al. (2011) and were not estimated (Table 1). The accuracy of the model and its parameters was evaluated using the relative error for each data point/set, the mean relative error (range 0 to ∞, zero describing a perfect fit) and the symmetrical mean squared error (range 0 to 1) for the entire model were calculated using the DEBtool.

2.3. Datasets

Data were collected from various experimental studies, encompassing a range of environmental conditions. Published datasets were used when available, and additional data were extracted from figures using the Rpackage metaDigitise (Pick et al., 2019; R Core Team, 2023). The collected datasets were integrated into the mydata file and standardized to match the units employed in DEB theory. In the predict file, the appropriate DEB equations were incorporated to compute each response variable. Adjustments were made to the pars_init file to accommodate new data specific parameters, including initial lengths, reproduction buffers, and functional responses (Appendix A). The full script is available on the Add-my-Pet database.

2.3.1. Zero-variate data

Zero-variate data refer to data consisting of single, point-specific values, such as measurements of size at birth or a specific age at maturity. Data for embryonic and larval development were obtained from Aranda-Burgos et al. (2014), who looked at the development of the clam between fertilization and settlement at 20 °C (Table 2). Additional comparisons of metamorphosis under different temperatures was possible due to experiments performed by Beiras et al. (1994) rearing larvae under different temperatures (10, 16, 22 and 28 °C). Notably, there is a discrepancy between the two studies: Aranda-Burgos et al. (2014) describe metamorphosis as occurring when the velum is shed and adult gills develop, as the clam settles at a size of 208 μm. However, Beiras et al. (1994) provide no additional explanation and assumes metamorphosis occurs at a specific length (240 μm), reporting the age at which this size is reached. Age and length at puberty were obtained from Pérez-Camacho (1980) and life span from Urrutia et al. (1999) who both looked at growth and reproduction of the grooved carpet shell. Lastly, daily egg production was obtained from Maynou et al. (2020).

Table 3
Uni-variate data, trend data containing a vector of dependent variables and associated independent variables, and relative errors (RE) from DEB model prediction of the grooved carpet shell, T: temperature, f: functional response.

Description	Groups	DEB notation	T	f	Units	RE
Wet weight vs. Length[b]		L-Ww	–	1	g - cm	0.07
Wet weight vs. Total length[c]		L-Ww	–	1	g - mm	0.04
Live weight vs. Length[d]		L-Ww	–	1	g - cm	0.15
Wet weight vs. Length[e]		L-Ww	–	0.5	g - cm	0.06
Length vs. Age[f]		t-L_T1	10 °C	0.85	µg - days	0.10
		t-L_T2	16 °C			0.07
		t-L_T3	22 °C			0.11
		t-L_T4	28 °C			0.11
Dry weight vs. Age[f]		t-Wd_T1	10 °C	0.85	µm - days	0.32
		t-Wd_T2	16 °C			0.10
		t-Wd_T3	22 °C			0.21
		t-Wd_T4	28 °C			0.31
Ingestion rate vs. Concentration[g]	Length: 108 µm	X-JX_L1	20 °C	–	g C h^{-1} - cells μl^{-1}	0.26
	Length: 172 µm	X-JX_L2		–		0.11
	Length: 196 µm	X-JX_L3		–		0.19
	Length: 226 µm	X-JX_L4		–		0.35
Ingestion rate vs. Wet weight[h]	*I. galbana*	Ww-JX_f1	20 °C	–	µg organic dry weight d^{-1} - g	0.19
	T. suecica	Ww-JX_f2		–		0.25
	P. tricornutum	Ww-JX_f3				0.19
Wet weight vs. Time[h]	*I. galbana*	t-Ww_f1	20 °C	0.79	mg - days	0.13
	T. suecica	t-Ww_f2		0.86		0.14
	P. tricornutum	t-Ww_f3		0.67		0.10
Length vs. days after fertilization[i]	Starvation	t-L_f1	22 °C	0	cm - days	0.03
	Isochrysis aff galbana	t-L_f2		0.44		0.05
	Chaetoceros calcitrans	t-L_f3		0.51		0.09
Length vs. Time since start experiment[j]		t-L	17.5 °C	0.69	cm - days	0.13
Tissue dry weight vs. Time since start experiment[k]	Age class 0	t-Wd_a0	[a]	[a]	g - days	0.21
	Age class 1	t-Wd_a1				0.22
	Age class 2	t-Wd_a2				0.10
	Age class 3	t-Wd_a3				0.07
	Age class 4	t-Wd_a4				0.07
	Age class 5	t-Wd_a5				0.06
	Age class 6	t-Wd_a6				0.06
Tissue dry weight vs. Time since start starvation[l]		t-Wd	17 °C	0	g - days	0.03
Length vs. Time since start experiment[d]	Location A	t-L_f1	[a]	0.96	cm - days	0.04
	Location B	t-L_f2		0.96		0.04
	Location C	t-L_f3		1		0.05
Weight vs. Time since start experiment[d]	Location A	t-Ww_f1	[a]	0.96	g - days	0.07
	Location B	t-Ww_f2		0.96		0.12
	Location C	t-Ww_f3		1		0.12
Change in shell length vs. Shell length[j]		L-dL	17.5 °C	0.69	cm d^{-1} - cm	0.38

[a] Variable.
[b] Pérez-Camacho (1980).
[c] Ojea et al. (2004).
[d] Erdal and Önal (2020).
[e] de Sousa et al. (2011).
[f] Beiras et al. (1994).
[g] Pérez-Camacho et al. (1994).
[h] Albentosa et al. (1996).
[i] Matias et al. (2011).
[j] Juric et al. (2012).
[k] Urrutia et al. (1999).
[l] Albentosa et al. (2007).

2.3.2. *Uni-variate data*

Uni-variate data, describing changes in size, ingestion and reproduction, were obtained from a range of studies gathering data or performing experiments on the grooved carpet shell (Table 3). Beiras et al. (1994) performed laboratory experiments looking at the effect of four temperatures, 10, 16, 22 and 28 °C, on the growth, ingestion, and clearance rates of the larvae, revealing that all rates increased linearly with increasing temperature. The data on growth were used to estimate the Arrhenius temperature. Additional data on growth were added to improve the estimation of the growth related parameters: shell length measurements in the eastern Adriatic Sea by Juric et al. (2012) and length and weight measurements from three locations in the Çanakkale strait in Turkey by Erdal and Önal (2020). Data to estimate the shape coefficient, containing length and weight data, were obtained from four studies, from Pérez-Camacho (1980), Erdal and Önal (2020), Ojea et al. (2004) and de Sousa et al. (2011). Matias et al. (2011) performed experiments measuring the change in length of larvae under three food conditions: 50 cells μl^{-1} *Isochrysis galbana* or *Chaetoceros calcitrans*, or no food at all at 22 °C. The change in length under three food conditions was modelled using the function developed by Augustine et al. (2011), who rewrote the functions in the model to more accurately describe allocation of energy and accommodate for a functional response of 0 (no food) for the zebrafish. Given the shared abj typified model of both zebrafish and the grooved carpet

shell, these functions were adapted to predict the grooved carpet shell's response to starvation. The same function was used to predict the change in weight for data from Albentosa et al. (2007) who measured the change in weight of the clam subject to starvation for 84 days. Albentosa et al. (1996) explored ingestion rates in relation to individual weight of grooved carpet shell larvae across three microalgal diets: *Isochrysis galbana, Tetraselmis suecica* and *Phaeodactylum tricornutum*, they fed the diets at concentration of 2% of live body weight per day and reported variation in absorption efficiency for each diets. The highest absorption efficiency in the experiment was found for *Isochrysis galbana* (88.6%), followed by *Tetraselmis suecica* (67.9%) and the lowest for *Phaeodactylum tricornutum* (56.9%). Lower absorption efficiencies were compensated by higher mean ingestion rates, particularly for *T. suecica* (168.6 μg AFDW ind^{-1} d^{-1}) compared to *P. tricornutum* (111.0 μg AFDW ind^{-1} d^{-1}), with the lowest ingestion rate observed for *I. galbana* (102.9 μg AFDW ind^{-1} d^{-1}). Using the estimation procedure, digestion efficiencies (κ_X), which in DEB theory is the fraction of ingested energy assimilated into the reserves, were determined for each diet. Pérez-Camacho et al. (1994) looked at the effect of food concentration on larvae of four different body sizes, they fed *Isochrysis galbana* in five concentrations (10, 50, 100, 200, 300 cells μl^{-1}) and measured ingestion rates. The ingestion rates were formatted from cells h^{-1} to g C h^{-1} using a rough approximation of 20 peta-gram C per microalgal cell (Pérez-Morales et al., 2015). The half-saturation constant was estimated, whereas the κ_X that was used for the estimation of ingestion of the *Isochrysis galbana* diet from Albentosa et al. (1996) was used here as well, contributing to the estimation of the value. The functional responses were estimated for the datasets from experiments using fixed food levels, which were from Albentosa et al. (1996, 2007), Matias et al. (2011), Ojea et al. (2004) and field experiments from Beiras et al. (1994), Erdal and Önal (2020) and Juric et al. (2012). A seasonally varying f was estimated for the dataset from Urrutia et al. (1999), who sampled the grooved carpet shell in the Urdaibai Estuary (Basque Country, Spain) from September 1987 to March 1989. The variable temperature was added using data from the World sea temperature website. Apart from the seasonal changes, Urrutia et al. (1999) also observed clear spawning events between July and August when the body mass of the clam noticeably declined. For this reason spawning is added to the formulations as a forcing function, as has been previously done by Rosland et al. (2009). We implemented a temperature and reproductive buffer threshold, which were both estimated using the estimation procedure, which after being met empties the reproduction buffer, mimicking spawning.

3. Methods: Interspecific comparison

3.0.1. Species characteristics

For comparison, next to the grooved carpet shell, six additional filter-feeding bivalve species were selected, all of which are commercially cultivated in Europe and have relevant parameters available: common mussel (*Mytilus edulis*), Mediterranean mussel (*Mytilus galloprovincialis)*, flat oyster (*Ostrea edulis*), Pacific oyster (*Magallana gigas*), common cockle (*Cerastoderma edule*), and great scallop (*Pecten maximus*). There are important distinctions among these species (Table 4). Most are temperate bivalves native to the Northern Atlantic; however, the Pacific oyster is an invasive species. The Mediterranean mussel, as its name suggests, occurs in warmer climates. The flat oyster is unique in being larviparous, meaning its eggs remain in the shell after fertilization and only leave after developing into larvae. Both oyster species, Ostrea edulis and Magallana gigas, utilize an 'asj' typified model which delays acceleration until a specified maturity level and are also hermaphroditic. The great scallop is also hermaphroditic and unique in its ability to spawn multiple times per year. While most of these species are epifaunal, living on the surface of substrates, the grooved carpet shell and common cockle are distinct burrowing species (infaunal).

3.1. Aquaculture related traits

Using the DEB model, various individual, or implied, traits can be calculated. Implied traits are available at the Add-my-Pet portal for all DEB entries and give predictions on, among other things, the age and size at life-history events, residence time of compounds in the reserve and fluxes of carbon, oxygen, nitrogen and heat during life-history. Implied traits and parameters were selected based on their effect on growth and reserve dynamics. The von Bertalanffy growth coefficient $\dot{r}_B$ (with the unit d^{-1}) indicates how quickly the growth rate decelerates, and where (assuming the same ultimate size) a higher value thus results in a steeper growth curve. The maximum reserve capacity $[E_m]$, also called maximum storage density, is the energetic content of the reserve in J cm^{-3} at optimal food conditions and a larger content enables an organism to pay maintenance for longer and resist starvation. The maximum surface specific assimilation rate $\{\dot{p}_{Am}\}$ (unit J d^{-1} cm^{-2}) represents the efficiency at which the organism can take up food from the environment. The volume-specific cost of growth $[E_G]$, is the parameter describing the energy needed to grow a specific volume of structure (J cm^{-3}). The parameter kappa (κ) describes the fraction of reserve energy allocated to growth and maintenance whereas 1-κ goes into maturation and reproduction. The Arrhenius temperature, in Kelvin, is the parameter used to calculate the temperature correction factor. A high Arrhenius temperature results in a large difference in rates between different temperatures. Lastly, the volume specific maintenance costs $[\dot{p}_M]$ are the costs to maintain a unit of body volume, J d^{-1} cm^{-3}, and combined with the reserve capacity it reflects the ability of an organisms to maintain its structure under low food conditions.

Using the script developed by Kooijman et al. (2020), incorporated in the so-called AmPtool (AmPtool), population traits were calculated for the grooved carpet shell. These traits are available for nearly all AmP entries and give insight into life-history traits and patterns in population growth potential. The population traits consist of yield coefficients of food, age and size structure, population doubling time, survival probabilities and stable age distributions. The yield coefficients include yield of food on, feces Y_P, (dead) structure Y_{Vd}, (dead) reserves Y_{Ed}, yield in carbon dioxide Y_C and nitrogenous waste Y_N. Using these yield coefficients the production-assimilation (P:A) ratio was calculated (van der Meer et al., 2024) which describes the efficiency of converting assimilated energy into biomass (structure and reserves): $PA = (Y_{Vd} + Y_{Ed})/(1 - Y_P)$. A high P:A ratio indicates a high production efficiency, where most of the assimilated energy is converted into biomass, whereas a low ratio indicates a low production efficiency and more energy lost to metabolic processes. Utilizing the data on population traits from the AmP database and the script from van der Meer et al. (2024), the P:A ratio was calculated for the grooved carpet shell and other relevant bivalve aquaculture species.

Additionally, we simulated all species using the AmP tool (function simu_my_pet) to predict the age at which they reach commercial size under three different food conditions ($f = 1$, $f = 0.75$, and $f = 0.5$) at 20 °C. Furthermore, we calculated the cumulative investment into reproduction and reserve size when they reach commercial size. Commercial size approximations were as follows: 3 cm for the grooved carpet shell (FAO, 2006), 6 cm for the flat oyster (Montes et al., 2003), 5 cm for the blue mussel (Fisheries and Oceans Canada, 2003), 7.5 cm for the Pacific oyster (FAO, 2024), 2 cm for the common cockle (Pronker et al., 2015), 10 cm for the great scallop (Bergh and Strand, 2001), and 8 cm for the Mediterranean mussel (FAO, 2009).

4. Results

4.1. Zero-variate data

Relative errors (RE) for age and length at metamorphosis were on the higher end, since the model underestimates the age at metamorphosis at 20 °C (RE: 0.22) whereas it overestimates the age at

Table 4
Bivalve aquaculture species characteristics.

Species	Grooved carpet shell	Blue mussel: Common	Blue mussel: Mediterranean	Flat oyster	Pacific oyster	Common cockle	Great scallop
	Ruditapes decussatus	*Mytilus edulis*	*Mytilus galloprovincialis*	*Ostrea edulis*	*Magallana gigas*	*Cerastoderma edule*	*Pecten maximus*
Area	Intertidal[e]	Intertidal & subtidal[c]	Intertidal & subtidal[f]	Inter-/sub- tidal[c]	Inter-/sub- tidal[c]	Inter-/sub- tidal[b]	Subtidal[g]
Lifestyle	infaunal[e]	Epifaunal, reef forming	Epifaunal[f]	Epifaunal	Epifaunal, reef forming	Infaunal	Epifaunal[g]
Substrate	Burrows in sand/silt[e]	Rock and sand	Rock, mud and sand[f]	Rock and sand[c]	Rock[c]	Burrows in sand/mud	Sand, sandy gravel[g]
Commercial size (cm)	3	5	8	6	7.5	2	10
Lifespan (years)	8	24	12	35	30	14	14
Spawning mode	Oviparous[e]	Oviparous[a]	Oviparous[f]	Larviparous[a]	Oviparous[a]	Oviparous[d]	Oviparous[a]
Reproduction strategy/sexual differentiation	Gonochoristic	Gonochoristic[a]	Gonochoristic[f]	Sequential hermaphroditism[a]	Consecutive hermaphroditism[a]	Gonochoristic[d]	Hermaphroditism[a]

[a] Helm et al. (2004).
[b] Pronker et al. (2015).
[c] van der Veer et al. (2006).
[d] Tyler-Walter (2007).
[e] Urrutia et al. (1999).
[f] FAO (2009).
[g] Bergh and Strand (2001).

metamorphosis at 28 °C (RE: 0.18) (Table 2). The size at metamorphosis is also overestimated (RE: 0.64), almost doubling the original value, indicating the need to further research the variability of metamorphosis and its dependency of temperature. Furthermore, the estimate for length at puberty is relatively accurate (RE: 0.06), and although age at puberty is less accurate with an overestimation (RE: 0.43) this is more acceptable given the inherent variability of puberty. The model performs well in estimating age at birth, egg size, daily egg production, ultimate length and life span (RE < 0.1) albeit with a slight overestimation of length at birth (RE: 0.13).

4.2. Uni-variate data

The increase in ingestion rate due to the increase in mass was well reproduced by the model, with *T. suecica* showing the highest ingestion rates, followed by *P. tricornutum* and *I. galbana* (Fig. 1a). The highest digestion efficiency was found for *I. galbana* (κ_X: 0.69), followed by *P. tricornutum* (κ_X: 0.55) and the lowest for *T. suesica* (κ_X: 0.47). The model prediction follows the general trend of the data but due to the high scatter the relative errors are quite high (Table 3). The predicted change in ingestion rate due to food concentration captures the general trend, however, the model fails to accurately predict the decrease in ingestion rates beyond a concentration of 200 cells μl^{-1} (Fig. 1b). Starvation in two experiments at 22 °C and 17 °C were predicted well (RE: <0.05), especially over longer times where the shrinkage due to somatic maintenance becomes visible (Fig. 1c and d).

Seasonal growth with varying temperature and food conditions were well reproduced (Fig. 2). The variation in growth rate was mainly determined by the functional response, and to a small extent by the variation in temperature. The lowest functional response value was observed at the end of winter/early spring (0.42), peaking in summer (1), dropping significantly in autumn (0.68), and declining slightly towards winter (0.63). Furthermore, the prominent dip in the prediction around 550 days corresponded to spawning events observed in the data, which was introduced in the model as a forcing function in which the reproduction buffer was completely depleted, resulting in a abrupt reduction in weight. However, in natural settings, spawning is influenced by various environmental factors such as food availability and temperature, as well as internal dynamics. This variability was evident in the observed data, where individuals spawned at different times, resulting in a more gradual decline in weight over time.

The change in shell length as a function of shell length shows a general trend of decreasing growth rate with increasing shell length which was reproduced by the model (Fig. 3). The large variability around the regression line, especially for juveniles (<2 cm), indicates that while shell length is a significant predictor of growth rate, other factors also influence the growth dynamics of the clam. The predicted trend suggests a linear decrease in growth rates with increasing shell length and predicts higher growth rates for larger sizes (>3.5 cm) than is observed in the data, suggesting a larger ultimate size when the growth rate becomes zero (≈4.7 cm). However, in the data growth slows down fast initially but becomes less steep for larger sizes in what appears to be a decay curve. This implies that clams can continue growing at larger sizes, where the growth rate becomes very low but not zero leading to a larger ultimate size.

The performance of the estimated parameters is measured by the alignment between observations and predictions and resulted in a mean relative error of 0.125 and a symmetrical mean squared error of 0.027 for the entire model.

4.3. Parameters

4.3.1. Shape coefficient

The three shape coefficients estimated for the grooved carpet shell were 1.74 for the egg, 1.19 for the larval stage and 0.59 for the juvenile and adult species and appeared accurate in predicting the length-weight relation for the four datasets (Fig. 4). The adult shape coefficient performed best for the length-weight data from locations in Spain and Portugal (RE: <0.1) and less for data from an estuary in Turkey (RE: 0.15), where a larger shape coefficient would have fitted the data better, indicating a less elongated shape. The decrease in shape coefficient from egg to adult reflects the change in relationship between physical length and structural volume in the model, since: $L_p = V^{(1/3)}/\delta_m$, indicating that adult species have a more elongated form compared to larvae. Lastly, the shape coefficient for the egg was estimated using the egg diameter (67.4 μm) which was accurately estimated as well with 68.5 μm (RE: <0.05).

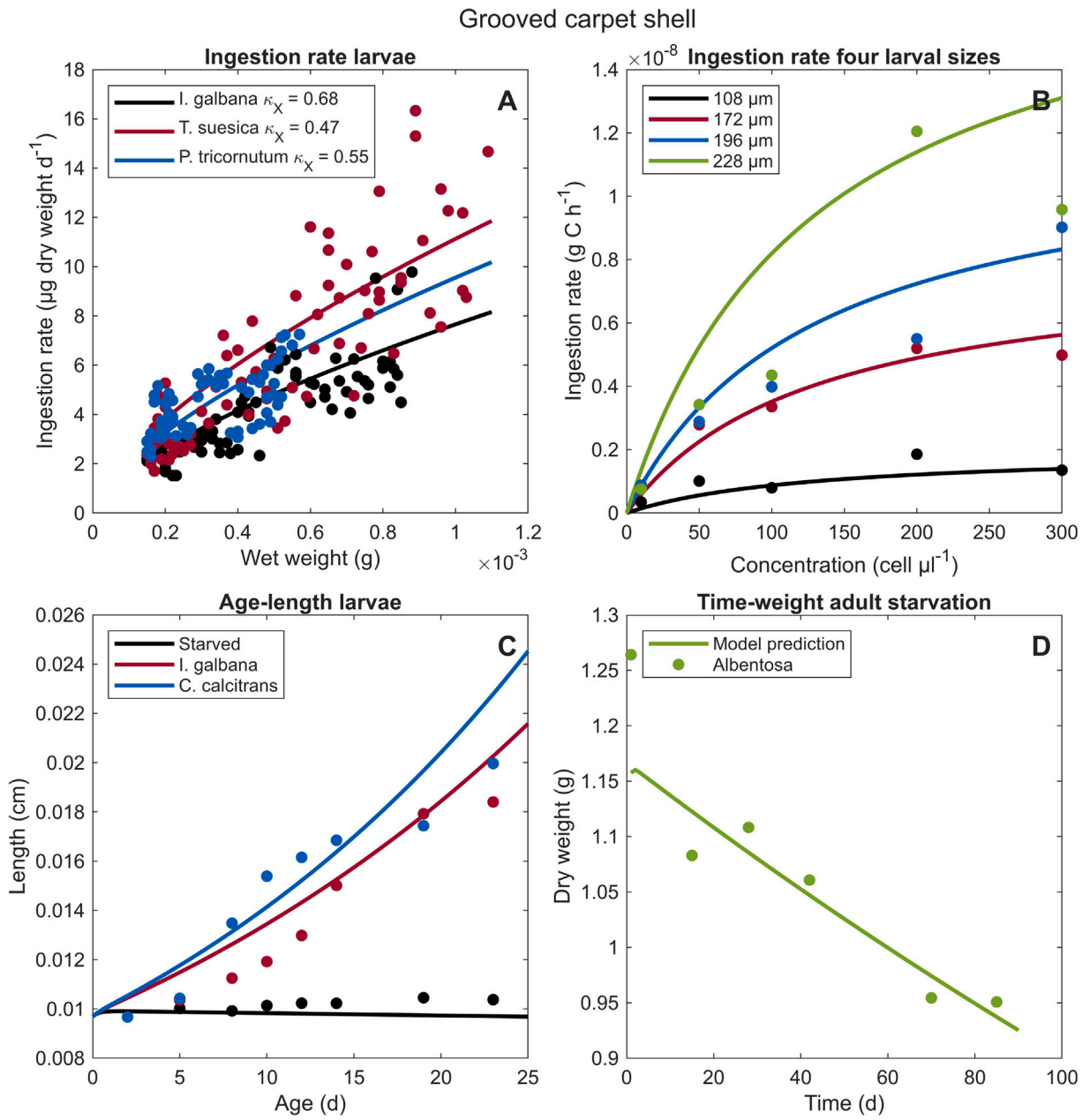

Fig. 1. DEB model predictions (lines) for the grooved carpet shell for ingestion, length and weight data (points) (A) ingestion rate for three diets (*I. galbana, T. suecica and P. tricornutum*) vs. clam live weight, experimental data obtained from Albentosa et al. (1996) (B) ingestion rates vs. algal cell concentration for four body sizes 228 µm, 196 µm, 172 µm and 108 µm, experimental data obtained from Pérez-Camacho et al. (1994) (C) length vs. age (time since fertilization) data for three diets started at day 2 (starvation, *Isochrysis aff galbana* and *Chaetoceros calcitrans*), experimental data obtained from Matias et al. (2011) (D) dry weight vs. time since start starvation, experimental data obtained from Albentosa et al. (2007).

4.4. Arrhenius temperature

Model simulations using the Arrhenius temperature partially captured the temperature response dynamics. An Arrhenius temperature of 3459 K was found to best predict growth changes due to temperature. All four temperature experiments started with clams of the same size, and conditioning at different temperatures led to differences in growth rates. Higher temperatures (up to 28 °C) resulted in increased growth rates which were much steeper in the model prediction, while the lowest temperature (10 °C) showed very low growth rates and high mortality, an effect that was not as pronounced in the model prediction (Fig. 5). While all rates increased with rising temperatures, the model's exponential temperature-growth rate relationship resulted in deviations from observed linear trends, particularly in age-weight predictions at higher temperatures.

4.5. Aquaculture related traits

The Von Bertalanffy coefficient is a growth parameter that indicates the rate at which an organism approaches its maximum size. The grooved carpet shell has a relatively low value (0.0007 d^{-1}), suggesting slower growth compared to other species, though even lower values were found for the blue mussel and Pacific oyster (0.0003 and 0.0004 d^{-1}, respectively), high values such as for the flat oyster (0.0015 d^{-1}) and the scallop (0.0021 d^{-1}) suggest steeper growth curves. The maximum reserve capacity represents the maximum amount of energy an organism can store under optimal food conditions and exhibits notable variation among the bivalve species. The Pacific oyster shows an exceptionally high value (14 469 J cm^{-3}), suggesting a high capacity for energy storage. In contrast, the grooved carpet shell and blue mussel

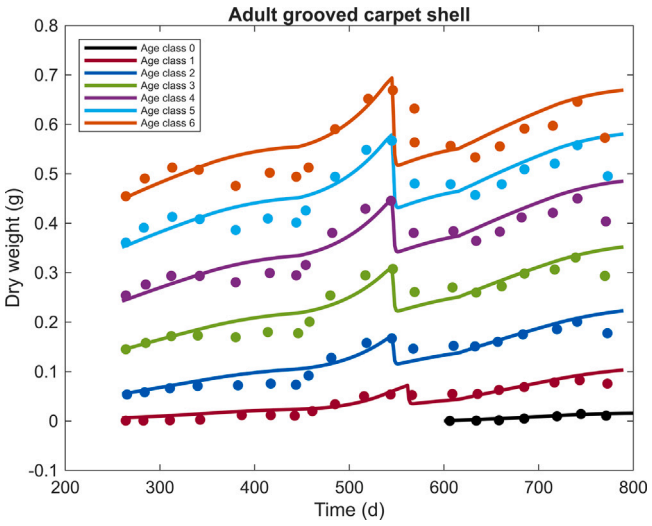

Fig. 2. Seasonal growth DEB model predictions (lines), dry weight vs. time, for the grooved carpet shell in Urdaibai Estuary (Basque Country. N. Spain), data (points) obtained from Urrutia et al. (1999), with spawning occurring when the reproduction threshold (903.4 J) is exceeded and temperatures are above 20 °C. Four functional responses were estimated per season: Spring: 0.42 Summer: 1.0 Autumn: 0.68 Winter: 0.63.

have much lower reserve capacities (208 and 181 J cm^{-3}), indicating limited energy storage capability. Volume–specific cost of structure measures the energy cost to build and maintain structural biomass and the values were relatively consistent across species, with slight variations. The grooved carpet shell (2346 J cm^{-3}) and blue mussel (2348 J cm^{-3}) are on the lower end, whereas the flat oyster (2392 J cm^{-3}) and scallop (2372 J cm^{-3}) have slightly higher costs. Kappa represents the fraction of energy allocated to maintenance and growth versus maturation and reproduction. The blue mussel has an exceptionally high kappa value (0.996), indicating nearly all energy is allocated to somatic processes, which leaves minimal energy for reproduction. The grooved carpet shell has a kappa value of 0.81, suggesting a more balanced allocation between somatic and reproductive efforts. The Pacific oyster and Mediterranean mussel have the lowest kappa values (0.26 and 0.48) which suggest low investment in growth and high energy allocation to reproductive efforts. The Arrhenius temperature parameter indicates the temperature sensitivity of metabolic rates. The Mediterranean mussel has the highest value (14 821.2 K), suggesting high sensitivity to temperature changes, whereas the grooved carpet shell has a much lower value (3459 K), indicating less sensitivity. The Arrhenius temperature values for both oyster (8000 K) is likely a reference value and not estimated. Volume-specific maintenance costs reflects the energy required for maintaining a unit volume of structure per day, combined with the maximum reserve density these reflect an organism's ability to withstand starvation. The scallop exhibits the highest maintenance costs (49.1 J d^{-1} cm^{-3}), while the blue mussel has the lowest (2.6 J d^{-1} cm^{-3}). The maximum surface-specific assimilation rate indicates the organisms ability to use the available food source. The Pacific oyster has the highest assimilation rate (77.60 J d^{-1} cm^{-2}), followed by the scallop (58.20 J d^{-1} cm^{-2}), whereas the Mediterranean mussel and grooved carpet shell have the lowest assimilation rates (7.13 and 6.72 J d^{-1} cm^{-2}) (see Table 5).

The production assimilation ratio is a measure of the efficiency of a species in converting assimilated energy into biomass (structure and reserves). P:A ratios for all AmP entries range from 1×10^{-7} to 0.99, with a mean of 0.07 which shows the extremely skewed distribution of the P:A ratio (Fig. 6a). The mean P:A for the bivalves is much higher with 0.12, ranging from 3×10^{-3} to 0.58 (Fig. 6b). Both the blue mussel (0.3344) and carpet shell (0.1898) have high P:A ratios, while both oyster species display low P:A ratios (≈0.01). The P:A ratios show a negative correlation with the von Bertalanffy growth coefficient (Fig. 7). Generally, bivalves show widespread variation in growth coefficient and P:A ratios. However, the species chosen here that share a native geographical range (mussels, carpet shell, cockle, flat oyster, and scallop) show similarity in growth coefficient and P:A ratio. Whereas the Pacific oyster, which is not native to the area, shows a lower growth coefficient and lower P:A ratio.

Age and energy investment at commercial size are relevant metrics to asses the trade-off between biomass production, growth rates and efficient energy allocation (Appendix B). The simulation suggest that the pacific oyster, scallop and Mediterranean mussel are the fastest growers with average growth rate higher than the other species. In contrast, the grooved carpet shell, blue mussel and common cockle have the lowest average growth rates (Fig. 8a). When examining the cumulative energy investment in reproduction per unit of volume, it is evident that the flat oyster, Pacific oyster, and Mediterranean mussel allocate significantly more energy towards reproduction. Conversely, the scallop, blue mussel, grooved carpet shell, and common cockle invest much less in reproduction (Fig. 8b).

5. Discussion

Overall, the DEB model successfully predicted the changes in weight, length, and ingestion over time for the grooved carpet shell under varying conditions of food availability and temperature. The accuracy of the model holds across diverse datasets from multiple geographical locations and laboratory conditions, confirming the robustness and predictive power of DEB theory in determining species-specific parameters. Yet, several datasets lacked the specific detail required for comprehensive DEB parameter estimation, as it was not initially collected with DEB modelling in mind. This limitation necessitated, for example, the estimation of critical steering factors such as food conditions.

5.1. Grooved carpet shell parametrization

Model predictions for ingestion rates, based on the experiment conducted by Albentosa et al. (1996), revealed a different order of the digestion efficiency parameter κ_X for the three diets (*I. galbana* > *P. tricornutum* > *T. suecica*) compared to reported absorption efficiencies (*I. galbana* > *T. suecica* > *P. tricornutum*), but aligned better with reported ingestion rates (*T. suecica* > *P. tricornutum* > *I. galbana*). This discrepancy between prediction and reality highlights that in DEB theory, low digestibility is only compensated by higher ingestion rates although in reality other processes such as selective ingestion and the concentration of indigestible particles also play a role (Prins et al., 1991). Further research is necessary to fully understand ingestion and assimilation processes, particularly in aquaculture where food conditions vary. Additionally, the grooved carpet shell exhibits distinct length-weight relationships across different geographical locations, such as the Çardak estuary in Turkey which shows different morphological characteristics compared to those from a basin in Spain and the Rio de Aveiro in Portugal (de Sousa et al., 2011; Erdal and Önal, 2020; Ojea et al., 2004; Pérez-Camacho, 1980). Such variation in morphology can be attributed to both genetic differences and phenotypic plasticity, where environmental factors can lead to different morphologies within the same species (Steeves, 2022). Significant morphological differences have been reported between populations from the Atlantic Ocean and the Mediterranean Sea, as well as within single bays (Costa et al., 2008; Ghozzi et al., 2022), suggesting that distinct environments and potential genetic divergence influence the development of the grooved carpet shell. Understanding the drivers of phenotypic variation is essential for enhancing knowledge of adaptive responses in bivalve populations and their implications for production and ecosystem dynamics. Lastly,

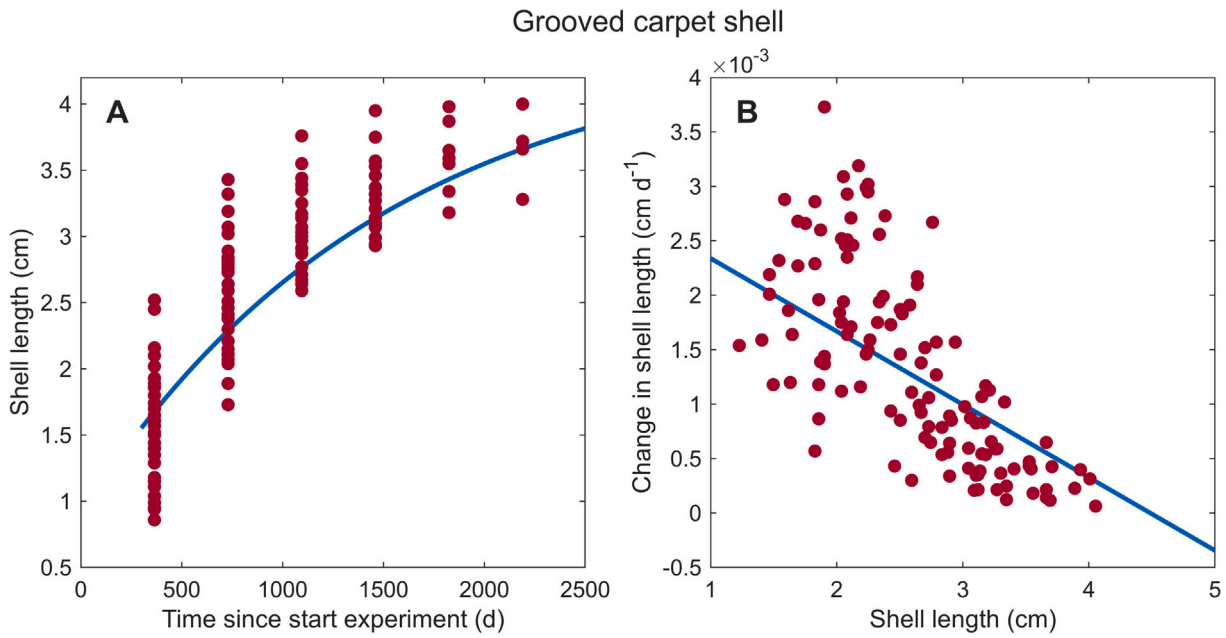

Fig. 3. Growth DEB model predictions (blue lines) of the grooved carpet shell in the Eastern Adriatic Sea, data (red points) obtained from Juric et al. (2012) (A) shell length vs. time (B) change in shell length vs. shell length.

Table 5
Parameters, implied properties, and population traits for 7 aquacultural species obtained from the AmP website.

Species	Compound parameter		Primary parameter					Trait
	Von Bertalanffy growth rate/coefficient	Maximum reserve capacity	Cost of growth/structure	Kappa	Arrhenius temperature	Volume specific maintenance costs	Maximum assimilation	Production assimilation ratio
	$\dot{r}_B$ d^{-1}	$[E_M]$ J cm^{-3}	$[E_G]$ J cm^{-3}	κ –	T_A K	$[\dot{p}_M]$ J d^{-1} cm^{-3}	$\{\dot{p}_{Am}\}$ J d^{-1} cm^{-2}	– –
Grooved carpet shell (*Ruditapes decussatus*)	7.2×10^{-4}	218.1	2346	0.806	3459	5.485	6.98	0.1898
Flat oyster (*Ostrea edulis*)	14.6×10^{-4}	931.1	2392.32	0.954	8000	14.4	18.30	0.0924
Blue mussel (*Mytilus edulis*)	3.0×10^{-4}	181.4	2348	0.996	7022	2.6	11.07	0.334
Pacific oyster (*Magallana gigas*)	3.6×10^{-4}	14 469.1	2374	0.264	8000	17.3	77.60	0.0101
Common cockle (*Cerastoderma edule*)	10.2×10^{-4}	1550.9	2353.29	0.969	5290	18.3	14.19	0.116
Scallop (*Pecten maximus*)	21.1×10^{-4}	1926.3	2372.03	0.887	7671.14	49.1	58.20	0.0427
Mediterranean mussel (*Mytilus galloprovincialis*)	12.0×10^{-4}	299.9	2380.62	0.477	14 821.2	9.0	7.13	0.0478

optimal temperature ranges for the grooved carpet shell differ depending on geographical origin as well as between larval and adult stages, as they have different metabolic demands and live in different environments (pelagic vs. benthic) (da Costa et al., 2020; Matias, 2013; Pérez-Camacho et al., 1994). This suggests that additional temperature tolerance parameters might be necessary depending on the organism's life stage and origin, although the extent of its impact on the accuracy of the prediction remains to be explored.

5.2. Species comparison and implications for aquaculture

To determine the suitability of various bivalve species for aquaculture, we compared the DEB primary/compound parameters and traits across seven bivalve species. While we expected to find similarities in traits among closely related species, our results revealed notable differences in energy utilization strategies that highlight the differences in their aquaculture potential. However, due to uncertainties in parameter estimation and the significant influence of environmental factors, direct translation of these parameters to real-world aquaculture scenarios is challenging. Consequently, our interpretation focuses on understanding how these parameters might influence their potential for aquaculture.

5.2.1. Growth efficiency

The efficiency with which an organism utilizes available energy for growth is captured in several key DEB parameters and traits. From the von Bertalanffy growth coefficient ($\dot{r}_B$), the cost for growth $[E_G]$ and allocation to growth (κ), we can infer an organism's strategy towards growth and reproduction. The maximum assimilation rate $\{\dot{p}_{Am}\}$ indicates the organism's capacity to utilize available food resources while the production-assimilation ratio (P:A) measures how efficiently assimilated energy is converted into biomass. The blue mussel (*Mytilus edulis*) demonstrates a strategy characterized by significant investment

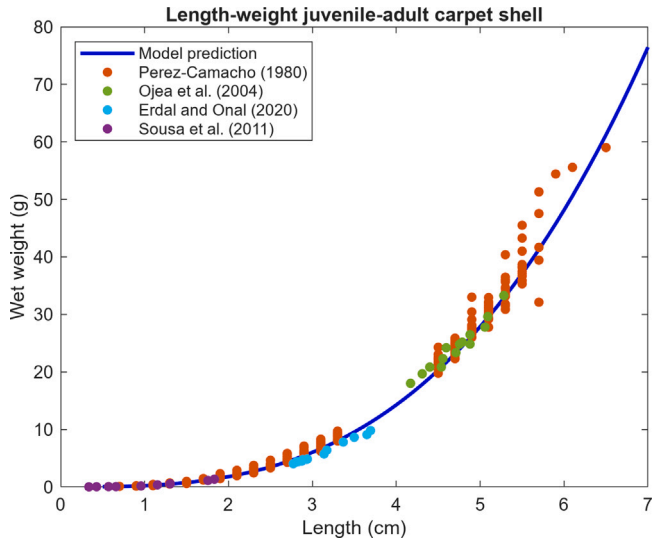

Fig. 4. Wet weight vs. length DEB model prediction (blue line) for the grooved carpet shell, field data (points) from Ria de Arousa (Spain) in orange obtained from Pérez-Camacho (1980), field data from Lagunas de Baldaio (Spain) in green obtained from Ojea et al. (2004), laboratory data with clams originating from Rio de Aveiro (Portugal) in purple obtained from de Sousa et al. (2011) and field data from Çardak estuary (Turkey) in light blue obtained from Erdal and Önal (2020).

in growth at the expense of reproduction, as shown by a high κ (0.99). The low $\dot{r}_B$ (0.0003 d^{-1}) and minimal maintenance costs (2.6 J d^{-1} cm^{-3}) result in the highest P:A ratio (0.334), which aligns with the theoretical expectation that low overhead costs and slow growth (compared to reproduction rate) lead to the highest production efficiency (van der Meer et al., 2024). Slow growth is demonstrated by the simulation predicting commercial size to be achieved relatively late (3.5–9.5 years), however, the slow growth rates found here contrast with field observations, which indicate much higher growth rates, particularly in warmer regions (Camacho et al., 1995). But even in temperate areas, commercial size can often be reached within two years (van Stralen and Dijkema, 1994), whereas the slow growth predicted by the model is more consistent with populations in the Baltic region (Kautsky, 1982). The flat oyster (*Ostrea edulis*) also prioritizes growth over reproduction (κ: 0.95). However, due to a high r_B (0.0015 d^{-1}), and substantial maintenance costs (14.4 J d^{-1} cm^{-3}), commercial size is attained more rapidly (2–4 years) at the cost of lower production efficiency (P:A: 0.092). In contrast, the Pacific oyster (*Magallana gigas*) and the Mediterranean mussel (*Mytilus galloprovincialis*) adopt a strategy that prioritizes reproductive investment over somatic growth as reflected in their low κ values (0.26 and 0.48, respectively). Still these species reach the commercial size relatively quickly (1–2 years for the Pacific oyster and 2–3 years for the Mediterranean mussel). Furthermore, it is important to note that in shellfish, the gonads are harvested along with the rest of the body, thereby contributing to the organism's total weight (Cho et al., 2023). However, the high investment in reproduction primarily benefits spat production and is mainly advantageous for harvest before the first spawning event. Despite having relatively low to moderate r_B values (0.00036 and 0.0012 d^{-1}, respectively) and average maintenance costs (17.3 and 9.05 J d^{-1} cm^{-3}), these species exhibit low P:A ratios (0.010 and 0.048), suggesting less efficient energy allocation strategies for biomass production. The scallop (*Pecten maximus*) demonstrates efficient utilization of available food and rapid growth, evidenced by its relatively fast growth to commercial size (10 cm in 2 years under optimal food conditions at 20 °C) and high assimilation rate (58.20 J d^{-1} cm^{-2}). However, the low production-assimilation (P:A) ratio (0.043) and high structural and maintenance costs (2372.03 and 49.1 J cm^{-3}) suggest a low efficiency in converting assimilated energy into biomass. The great scallop grows rapidly, especially under optimal conditions; however, its growth is significantly hindered by low food availability or temperatures. This is reflected in its inability to reach a commercial size of 10 cm at a functional response of 0.5 and its relatively high Arrhenius temperature (7671 K), which aligns with findings on its sensitivity to low temperatures (Bergh and Strand, 2001). Lastly, the common cockle (*Cerastoderma edule*) and grooved carpet shell (*Ruditapes decussatus*) show a more balanced growth strategy, characterized by moderate r_B (0.0010 d^{-1} and 0.0007 d^{-1}, respectively) and assimilation rates (14.19 and 6.98 J d^{-1} cm^{-2}, respectively). The cockle has a notably higher κ (0.97 vs. 0.81) and maintenance costs (18.3 vs. 5.5 J d^{-1} cm^{-3}). Both species reach commercial size relatively fast (1–2.5 years for the cockle and 2–4 for the carpet shell), mainly due to the smaller commercial sizes (2 and 3 cm), but combined with high P:A ratios (0.12 and 0.19) these species are interesting candidates for aquaculture.

5.2.2. Reserve and maintenance processes

Species that can efficiently store and allocate energy are more resilient to fluctuating food conditions and have the potential to resist starvation for longer periods, which are advantageous traits in both aquaculture and natural systems. The Pacific oyster has an exceptionally high maximum storage density (14 469.1 J cm^{-3}), combined with moderate maintenance costs, indicating strong resistance to starvation and an ability to thrive under fluctuating food conditions. Due to its high assimilation rate (77.60 J d^{-1} cm^{-2}), the oyster can quickly fill its reserves to survive low food conditions. This is supported by literature as the pacific oyster's resistance to starvation is notable. Larvae experience minimal mortality over 8 days of starvation, due to their buffering capacity from lipid reserves, and the immediate decrease of metabolic rates during starvation (García-Esquivel et al., 2002). Adult Pacific oysters starved up to 80 days showed less than 4% mortality by decreasing metabolic rates, although they undergo physiological changes that reduce immune capacity and delay post-spawning recovery (Li et al., 2009). Remarkably, Pacific oysters have even been documented to survive up to 400 days without food (Whyte et al., 1990). The second and third largest reserves are found in the scallop and common cockle (1926.34 and 1550.9 J cm^{-3}, respectively). However, these species differ greatly in maintenance costs (49.1 vs. 18.3 J d^{-1} cm^{-3}), making the scallop comparatively more susceptible to starvation. On the other hand, the low assimilation rate of the cockle makes it more difficult to refill its reserves in short periods of time, whereas the scallop shows one of the highest assimilation rates. The common cockle decreases their metabolic rate during winter when food and temperatures are low, often ceasing feeding altogether (Newell and Bayne, 1980). This adaptation allows them to avoid the cost of processing large amounts of food with little nutritional benefit, unlike for instance the blue mussel, which increase filtration rates and produces large amounts of pseudofeces in similar conditions. This seasonal dormancy in cockles is compensated by high feeding and absorption efficiency during more favourable conditions, when reserves are restored for winter survival. The flat oyster has a moderate storage density and moderate maintenance costs, allowing it some resistance to low food conditions but making it more sensitive in the long term. Lastly, the grooved carpet shell, common blue mussel, and Mediterranean mussel have low reserve densities (218.1, 181.43, and 299.93 J cm^{-3}, respectively) and low maintenance costs (5.485, 2.6, and 9.05 J d^{-1} cm^{-3}, respectively), making these species less resistant to long-term low food conditions. While their low maintenance costs allow them to withstand short periods of limitation, their low assimilation rates (6.98, 11.07 and 7.13 J d^{-1} cm^{-2}) mean they need comparatively longer periods of sufficient food to replenish their reserves. During starvation, these species can reduce their metabolic rates. However, the high growth rates and filtration capacity of the mussels lead to increased metabolic demands during low food conditions (Prieto et al., 2018). The grooved carpet shell, although quickly depleting its carbohydrate reserves, uses lipids more conservatively (Albentosa et al., 2007). Notably, despite

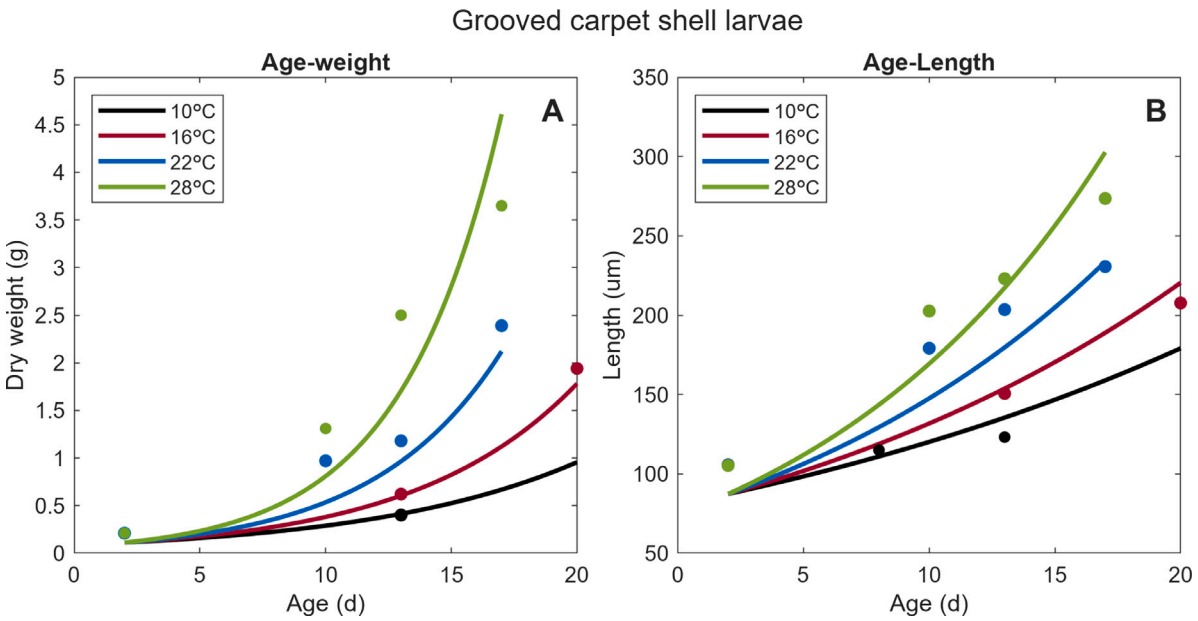

Fig. 5. DEB model predictions (lines) for the grooved carpet shell larvae, experimental data (points) for four temperatures (10, 16, 22 and 28 °C) obtained from Beiras et al. (1994): (A) dry weight vs. age data (B) length vs. age data.

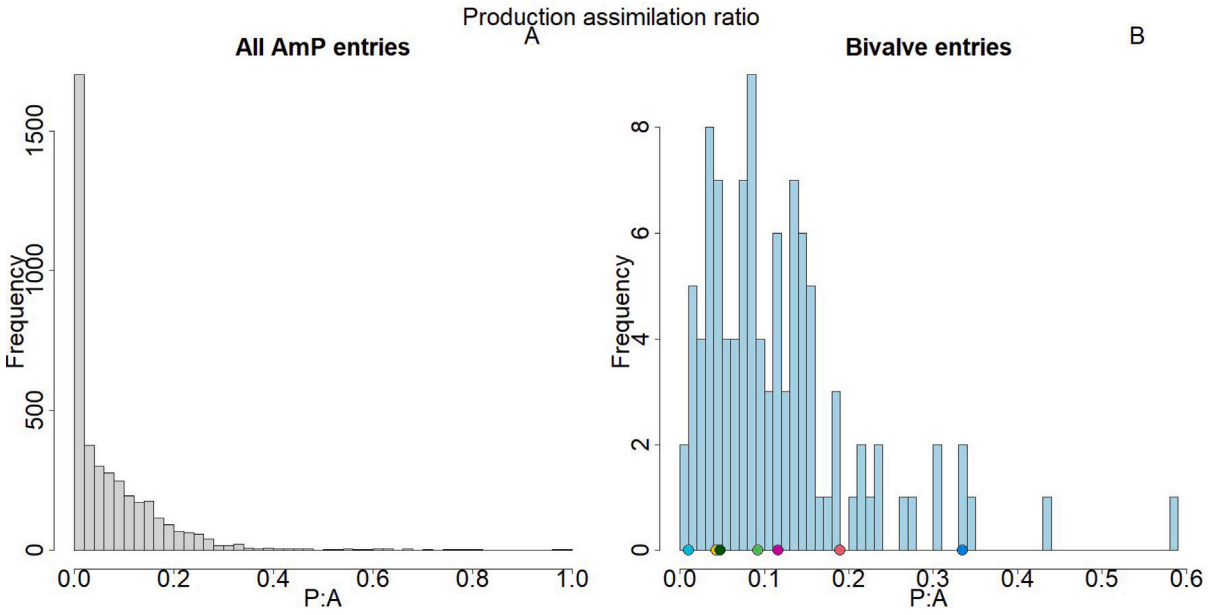

Fig. 6. Histogram of production assimilation ratio for (A) all AmP entries, (B) all bivalve entries with the aquacultural species as circles, the grooved carpet shell (red), flat oyster (green), blue mussel (dark blue), Pacific oyster (light blue), common cockle (purple), scallop (yellow) and Mediterranean mussel (darkgreen).

being more susceptible than other species, mussels have been shown to survive at least 80 days under starvation, and the grooved carpet shell for at least 84 days (Harbach and Palm, 2018; Albentosa et al., 2007).

5.2.3. Environment

Higher assimilation rates indicate a greater ability to utilize available food resources, promoting faster growth. However, assimilation rates are diet-dependent and therefore also influenced by location and temperature. Different locations provide varying qualities and quantities of food and temperature affects metabolic rates. These insights are crucial in understanding species-specific responses to environmental changes and for optimizing aquaculture practices. The diet-dependency in rates, as shown here for the grooved carpet shell, further emphasizes the importance of environmental factors, such as location and temperature, in determining the success of aquaculture species.

6. Concluding remarks

Among the species examined, the grooved carpet shell demonstrates a balanced strategy in energy allocation, with a mean kappa value, moderate growth coefficient, and temperature sensitivity, leading to relatively high production efficiency. Alternative strategies are observed in species such as the flat oyster (*Ostrea edulis*) and common cockle (*Cerastoderma edule*), which invest more energy in growth at the expense of reproduction. Conversely, the Pacific oyster (*Crassostrea gigas*) and Mediterranean mussel (*Mytilus galloprovincialis*) shows a

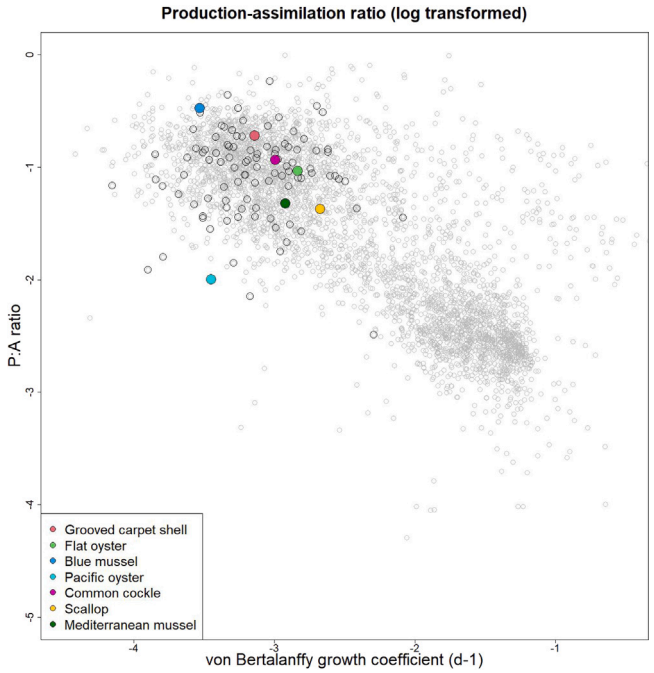

Fig. 7. Production assimilation ratio vs. the von Bertalanffy growth coefficient for all AmP entries (grey circles), black circles represent all entries in the Bivalvia class with the aquacultural species highlighted, the grooved carpet shell (red), flat oyster (green), blue mussel (dark blue), Pacific oyster (light blue), common cockle (purple), scallop (yellow) and Mediterranean mussel (darkgreen).

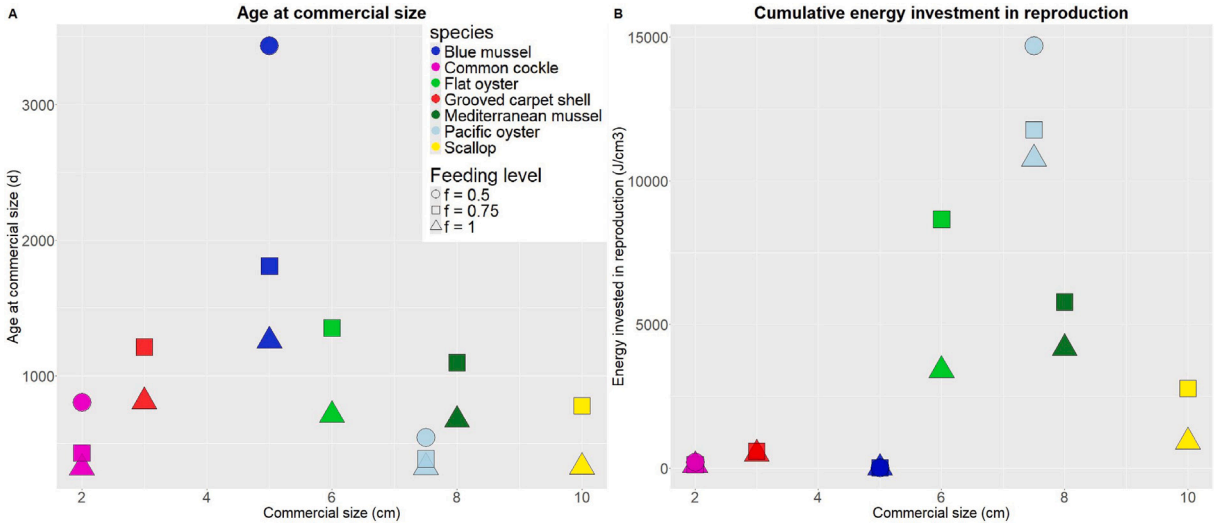

Fig. 8. Age and reproductive investment at commercial size for seven bivalve aquaculture species at three different functional responses (1, 0.75 and 0.5) and 20 °C, (A) age at commercial size (B) cumulative energy investment into reproduction per unit of body volume.

higher investment in reproduction at the cost of growth and production efficiency. The blue mussel (*Mytilus edulis*) demonstrates a strategy with high investment in growth, resulting in high production efficiency due to lower maintenance rates. Lastly, the scallop (*Pecten maximus*) appears to have a balanced strategy but with a moderate growth coefficient and high maintenance costs, resulting in lower production efficiency. Bivalves generally display a high production efficiency, making them a sustainable and viable option in food production, with the blue mussel and grooved carpet shell emerging as the most efficient species among those examined. Overall, robust individual-based models such as DEB hold promise for informing future ecosystem modelling endeavors and optimizing sustainable aquaculture practices and ecosystem management strategies, especially in the context of changing climatic and socio-economic conditions.

CRediT authorship contribution statement

Merel Lanjouw: Writing – original draft, Visualization, Validation, Methodology, Formal analysis, Data curation. **Henrice M. Jansen:** Writing – review & editing, Supervision, Funding acquisition, Conceptualization. **Jaap van der Meer:** Writing – review & editing, Supervision, Methodology, Conceptualization.

Declaration of competing interest

The authors declare that they have no known competing financial interests or personal relationships that could have appeared to influence the work reported in this paper.

Data availability

No original data was used, the scripts will be made publicly available on the Add-my-Petwebsite.

Declaration of Generative AI and AI-assisted technologies in the writing process

During the preparation of this work the authors used OpenAI's ChatGPT 3.5 in order to improve readability and language. After using this service, the authors reviewed and edited the content as needed and take full responsibility for the content of the publication.

Acknowledgements

The authors would like to thank Bas Kooijman for his valuable feedback on the script and help performing the population trait calculation on the renewed scripts. The authors would also like to thank two anonymous reviewers for their helpful comments on the manuscript.

Funding

This publication is part of the project CircAqua with file number (KICH1.LWV01.20.003) of the research programme Aquatic Food production which is financed by the Dutch Research Council (NWO), The Netherlands.

Appendix A. Data specific parameters

See Table A.6.

Appendix B. Species simulations

See Table B.7.

Table A.6
Dataset specific parameter values for the DEB model of the grooved carpet shell.

Parameter	Units	Value	Description
E_{R01}	J	0	Initial reprod buffer in Urrutia et al. (1999) data age class 1
E_{R02}	J	0	Initial reprod buffer in Urrutia et al. (1999) data age class 2
E_{R03}	J	182.3	Initial reprod buffer in Urrutia et al. (1999) data age class 3
E_{R04}	J	97.89	Initial reprod buffer in Urrutia et al. (1999) data age class 4
E_{R05}	J	730.3	Initial reprod buffer in Urrutia et al. (1999) data age class 5
E_{R06}	J	1118	Initial reprod buffer in Urrutia et al. (1999) data age class 6
E_{Spawn}	J	903.4	Threshold in reproduction for spawning in Urrutia et al. (1999) data
$Kperez$	cells/µl	128.4	Half saturation concentration (Pérez-Camacho et al., 1994) data
L_0Urr0	cm	3.47×10^{-9}	Initial struct length (Urrutia et al., 1999) data
L_0Urr01	cm	0.4054	Initial struct length (Urrutia et al., 1999) data age class 1
L_0Urr02	cm	0.8267	Initial struct length (Urrutia et al., 1999) data age class 2
L_0Urr03	cm	1.12	Initial struct length (Urrutia et al., 1999) data age class 3
L_0Urr04	cm	1.351	Initial struct length (Urrutia et al., 1999) data age class 4
L_0Urr05	cm	1.49	Initial struct length (Urrutia et al., 1999) data age class 5
L_0Urr06	cm	1.606	Initial struct length (Urrutia et al., 1999) data age class 6
L_0Alb	cm	0.03781	Initial length for Albentosa et al. (2007) data
L_0Alb1	cm	0.05076	Initial length for Albentosa et al. (1996) data
L_0Chi	cm	0.008752	Initial length for Chícharo and Chícharo (2001) data
L_0Erdal	cm	2.6	Initial length for Erdal and Önal (2020) data
L_0Juric	cm	0.8984	Initial length for Juric et al. (2012) data
$L_0Matias$	cm	0.01154	Initial length for Matias et al. (2011) data
T_{Spawn}	K	293.4	Threshold in temp for spawning for Urrutia et al. (1999) data
f	–	1	Scaled functional response
f_{Alb}	–	1	Scaled functional response for Albentosa et al. (2007) data
f_{Alb1}	–	0.7908	Scaled functional response for Albentosa et al. (1996) data food type 1
f_{Alb2}	–	0.86	Scaled functional response for Albentosa et al. (1996) data food type 2
f_{Alb3}	–	0.6669	Scaled functional response for Albentosa et al. (1996) data food type 3
f_{Beir}	–	0.85	Scaled functional response for Beiras et al. (1994) data
f_{Cam}	–	1	Scaled functional response for Pérez-Camacho (1980) data
f_{Chi}	–	0.3147	Scaled functional response for Chícharo and Chícharo (2001) data
f_{Erdal}	–	1	Scaled functional response for Erdal and Önal (2020) shape data
f_{Erdal1}	–	0.9	Scaled functional response for Erdal and Önal (2020) data location SA
f_{Erdal2}	–	0.91	Scaled functional response for Erdal and Önal (2020) data location SB
f_{Erdal3}	–	0.96	Scaled functional response for Erdal and Önal (2020) data location SC
f_{Juric}	–	0.66	Scaled functional response for Juric et al. (2012) data
$f_{Matias1}$	–	0.4344	Scaled functional response for Matias et al. (2011) food type 1 data
$f_{Matias2}$	–	0.5067	Scaled functional response for Matias et al. (2011) food type 2 data
f_{Ojea}	–	1	Scaled functional response for Ojea et al. (2004) data
f_{Sousa}	–	0.5079	Scaled functional response for de Sousa et al. (2011) data
f_{UrrAut}	–	0.68	Scaled functional response for Urrutia et al. (1999) data in autumn
f_{UrrSpr}	–	0.42	Scaled functional response for Urrutia et al. (1999) data in spring
f_{UrrSum}	–	1	Scaled functional response for Urrutia et al. (1999) data in summer
f_{UrrWin}	–	0.63	Scaled functional response for Urrutia et al. (1999) data in winter

Table B.7
DEB growth simulations for seven bivalve aquaculture species at 20 °C for three food conditions (f = 1, 0.75 and 0.5).

Species	Commercial size	Age at size	Reserve	Cumulative energy reproduction	f
	cm	d	J	J	–
Grooved carpet shell	3	810	1187	2713	1
Flat oyster	6	710	2816	1865	1
Blue mussel	5	1258	900.91	56.9706	1
Pacific oyster	7.5	324	46 134	34 533	1

(continued on next page)

Table B.7 (*continued*).

Species	Commercial size	Age at size	Reserve	Cumulative energy reproduction	f
	cm	d	J	J	–
Common cockle	2	320	552	36	1
Scallop	10	326	71 991	34 148	1
Mediterranean mussel	8	674	1877	26 202	1
Grooved carpet shell	3	1211	890	3217	0.75
Flat oyster	6	1351	2123	4739	0.75
Blue mussel	5	1808	677	66	0.75
Pacific oyster	7.5	387	34 619	37 778	0.75
Common cockle	2	429	412	44	0.75
Scallop	10	778	53 855	103 374	0.75
Mediterranean mussel	8	1096	1404	36 324	0.75
Grooved carpet shell	3				0.5
Flat oyster	6				0.5
Blue mussel	5	3434	452	96.8	0.5
Pacific oyster	7.5	546	23 237	47 155	0.5
Common cockle	2	804	276	77	0.5
Scallop	10				0.5
Mediterranean mussel	8				0.5

References

Albentosa, M., Fernández-Reiriz, M.J., Labarta, U., Pérez-Camacho, A., 2007. Response of two species of clams, Ruditapes decussatus and venerupis pullastra, to starvation: Physiological and biochemical parameters. Comp. Biochem. Physiol. B 146 (2), 241–249. http://dx.doi.org/10.1016/j.cbpb.2006.10.109.

Albentosa, M., Pérez-Camacho, A., Beiras, R., 1996. The effect of food concentration on the scope for growth and growth performance of Ruditapes decussatus (L.) seed reared in an open-flow system. Aquacult. Nutr. 2, 213–220. http://dx.doi.org/10.1111/j.1365-2095.1996.tb00062.x.

Aranda-Burgos, J.A., Da Costa, F., Nóvoa, S., Ojea, J., Martínez-Patiño, D., 2014. Embryonic and larval development of Ruditapes decussatus (Bivalvia: Veneridae): a study of the shell differentiation process. J. Mollusc. Stud. 80 (1), 8–16. http://dx.doi.org/10.1093/mollus/eyt044.

Augustine, S., Litvak, M.K., Kooijman, S., 2011. Stochastic feeding of fish larvae and their metabolic handling of starvation. J. Sea Res. 66 (4), 411–418. http://dx.doi.org/10.1016/j.seares.2011.07.006.

Beiras, R., Camacho, A.P., Albentosa, M., 1994. Influence of temperature on the physiology of growth in ruditapes decussatus (L) larvae. J. Shellfish Res. 13, 77–83.

Bergh, Ø., Strand, Ø., 2001. Great scallop, Pecten maximus, research and culture strategies in Norway: a review. Aquac. Int. 9 (4), 305–317. http://dx.doi.org/10.1023/A:1020452715518.

Camacho, A., Labarta, U., Beiras, R., 1995. Growth of mussels (Mytilus edulis galloprovincialis) on cultivation rafts: influence of seed source, cultivation site and phytoplankton availability. Aquaculture 138 (1), 349–362. http://dx.doi.org/10.1016/0044-8486(95)01139-0.

Campbell, B.M., Beare, D.J., Bennett, E.M., Hall-Spencer, J.M., Ingram, J.S.I., Jaramillo, F., Ortiz, R., Ramankutty, N., Sayer, J.A., Shindell, D., 2017. Agriculture production as a major driver of the Earth system exceeding planetary boundaries. Ecol. Soc. 22 (4), 8, https://www.jstor.org/stable/26798991.

Cardoso, J.F.M.F., Witte, J.I.J., van der Veer, H.W., 2006. Intra- and interspecies comparison of energy flow in bivalve species in dutch coastal waters by means of the Dynamic Energy Budget (DEB) theory. J. Sea Res. 56 (2), 182–197. http://dx.doi.org/10.1016/j.seares.2006.03.011.

Chary, K., van Riel, A.-J., Muscat, A., Wilfart, A., Harchaoui, S., Verdegem, M., Filgueira, R., Troell, M., Henriksson, P.J.G., de Boer, I.J.M., Wiegertjes, G.F., 2023. Transforming sustainable aquaculture by applying circularity principles. Rev. Aquaculture 1–18. http://dx.doi.org/10.1111/raq.12860.

Chícharo, L., Chícharo, M., 2001. Effects of environmental conditions on planktonic abundances, benthic recruitment and growth rates of the bivalve mollusc Ruditapes decussatus in a Portuguese coastal lagoon. Fish. Res. 53 (3), 235–250. http://dx.doi.org/10.1016/S0165-7836(00)00290-3.

Cho, I.K., Seo, B.-S., Hwang, S.-Y., Lee, Y.-I., Moon, J.-S., Park, S.-J., Lee, H.-J., Hur, Y.B., Choi, Y.H., 2023. The annual reproductive cycle, proximate composition, fatty acid and amino acid content of Pacific oyster, crassostrea gigas (magallana gigas), in gadeok-do, Korea. Dev. Reprod. 27 (3), 101–115. http://dx.doi.org/10.12717/dr.2023.27.3.101.

Costa, C., Aguzzi, J., Menesatti, P., Antonucci, F., Rimatori, V., Mattoccia, M., 2008. Shape analysis of different populations of clams in relation to their geographical structure. J. Zool. 276 (1), 71–80. http://dx.doi.org/10.1111/j.1469-7998.2008.00469.x.

da Costa, F., Cerviño-Otero, A., Iglesias, Ó., Cruz, A., Guévélou, E., 2020. Hatchery culture of European clam species (family Veneridae). Aquac. Int. 28 (4), 1675–1708. http://dx.doi.org/10.1007/s10499-020-00552-x.

de Sousa, J.T., Matias, D., Joaquim, S., Ben-Hamadou, R., Leitão, A., 2011. Growth variation in bivalves: New insights into growth, physiology and somatic aneuploidy in the carpet shell Ruditapes decussatus. J. Exp. Mar. Biol. Ecol. 406 (1), 46–53. http://dx.doi.org/10.1016/j.jembe.2011.06.001.

Erdal, H., Önal, U., 2020. The growth and survival of carpet clam, ruditapes decussatus in Çardak Estuary (Çanakkale Strait, Northwest Turkey). Çanakkale Onsekiz Mart Univ. J. Mar. Sci. Fish. 3 (2), 120–129. http://dx.doi.org/10.46384/jmsf.822386.

FAO, 2006. Ruditapes decussatus. Cultured aquatic species information programme. text by Figueras, A.. https://www.fao.org/fishery/en/culturedspecies/ruditapes_decussatus/en.

FAO, 2009. Mytilus galloprovincialis. https://www.fao.org/fishery/docs/DOCUMENT/aquaculture/CulturedSpecies/file/en/en_mediterraneanmussel.htm.

FAO, 2024. Magallana gigas (Thunberg 1793). Tech. Rep., Cultured Aquatic Species Information Programme. Text by Helm, M.M., Rome.

Fisheries and Oceans Canada, 2003. Profile of the Blue Mussel (Mytilus edulis) Gulf Region Policy and Economics Branch, Gulf Region Department of Fisheries and Oceans Moncton, New Brunswick. Tech. Rep..

García-Esquivel, Z., Bricelj, V., Felbeck, H., 2002. Metabolic depression and whole-body response to enforced starvation by Crassostrea gigas postlarvae. Comp. Biochem. Physiol. A 133 (1), 63–77. http://dx.doi.org/10.1016/S1095-6433(02)00112-5.

Ghozzi, K., Dhiab, R.B., Challouf, R., Bradai, M.N., 2022. Morphometric variation among four local ruditapes decussatus populations in monastir bay (Eastern Coast, Tunisia). Agric. Agribusiness Biotechnol. 65, http://dx.doi.org/10.1590/1678-4324-2022210235.

Harbach, H., Palm, H., 2018. Development of general condition and flesh water content of long-time starved mytilus edulis-like under experimental conditions. Aquac. Aquarium Conserv. Legislation Bioflux 11, 301–308.

Helm, M., Bourne, N., Lovatelli, A., 2004. The Hatchery Culture of Bivalves: a Practical Manual. Tech. Rep., FAO, No. 471. Rome.

Inglis, G.J., Hayden, B.J., Ross, A.H., 2002. An Overview of Factors Affecting the Carrying Capacity of Coastal Embayments for Mussel Culture. Tech. Rep., Ministry for the Environment, Christchurch, https://api.semanticscholar.org/CorpusID:161051276.

Jansen, H.M., Van Den Burg, S., Bolman, B., Jak, R.G., Kamermans, P., Poelman, M., Stuiver, M., 2016. The feasibility of offshore aquaculture and its potential for multi-use in the North Sea. Aquac. Int. 24 (3), 735–756. http://dx.doi.org/10.1007/s10499-016-9987-y.

Juric, I., Bušelić, I., Ezgeta Balic, D., Vrgoc, N., Peharda, M., 2012. Age, growth and condition index of Venerupis decussata (Linnaeus, 1758) in the Eastern Adriatic Sea. Turk. J. Fish. Aquat. Sci. 12, 431–436. http://dx.doi.org/10.4194/1303-2712-v12{_}3{_}08.

Kautsky, N., 1982. Growth and size structure in a baltic Mytilus edulis population. Mar. Biol. 68 (2), 117–133. http://dx.doi.org/10.1007/BF00397599.

Koehn, J.Z., Allison, E.H., Golden, C.D., Hilborn, R., 2022. The role of seafood in sustainable diets. Environ. Res. Lett. 17 (3), 035003. http://dx.doi.org/10.1088/1748-9326/ac3954.

Kooijman, S., 2000. Dynamic Energy and Mass Budgets in Biological Systems, Ed 2. Tech. Rep., Cambridge University Press, Cambridge, http://dx.doi.org/10.1017/CBO9780511565403.

Kooijman, S., 2010. Dynamic Energy Budget Theory for Metabolic Organisation, third ed. Cambridge University Press, Cambridge, https://www.bio.vu.nl/thb/research/bib/Kooy2010.pdf.

Kooijman, S., Lika, K., Augustine, S., Marn, N., Kooi, B.W., 2020. The energetic basis of population growth in animal kingdom. Ecol. Model. 428, 109055. http://dx.doi.org/10.1016/j.ecolmodel.2020.109055.

Lavaud, R., Flye-Sainte-Marie, J., Jean, F., Emmery, A., Strand, Ø., Kooijman, S.A.L.M., 2014. Feeding and energetics of the great scallop, Pecten maximus, through a DEB model. J. Sea Res. 94, 5–18. http://dx.doi.org/10.1016/j.seares.2013.10.011.

Lavaud, R., Jolivet, A., Rannou, E., Jean, F., Strand, Ø., Flye-Sainte-Marie, J., 2019. What can the shell tell about the scallop? Using growth trajectories along latitudinal and bathymetric gradients to reconstruct physiological history with DEB theory. J. Sea Res. 143, 193–206. http://dx.doi.org/10.1016/j.seares.2018.04.001.

Li, Y., Qin, J.G., Li, X., Benkendorff, K., 2009. Spawning-dependent stress response to food deprivation in Pacific oyster Crassostrea gigas. Aquaculture 286 (3), 309–317. http://dx.doi.org/10.1016/j.aquaculture.2008.09.035.

Lika, K., Kearney, M.R., Freitas, V., van der Veer, H.W., van der Meer, J., Wijsman, J.W.M., Pecquerie, L., Kooijman, S., 2011. The "covariation method" for estimating the parameters of the standard Dynamic Energy Budget model I: Philosophy and approach. J. Sea Res. 66 (4), 270–277. http://dx.doi.org/10.1016/j.seares.2011.07.010.

Lopes, I., 2017. AmP ruditapes decussatus.

Machado, D., Baptista, T., Joaquim, S., Anjos, C., Mendes, S., Matias, A., Matias, D., 2018. Reproductive cycle of the European clam Ruditapes decussatus from Óbidos Lagoon, Leiria, Portugal. Invertebr. Repr. Dev. 62, http://dx.doi.org/10.1080/07924259.2018.1472671.

Marques, G., Augustine, S., Lika, K., Pecquerie, L., Domingos, T., Kooijman, S., 2018. The AmP project: Comparing species on the basis of dynamic energy budget parameters. PLoS Comput. Biol. 14 (5), e1006100. http://dx.doi.org/10.1371/journal.pcbi.1006100.

Matias, D., 2013. Establishment of Environmental and Biological Bases to Optimise the Production of the European Clam Ruditapes decussatus (Linnaeus, 1758) (Doctoral dissertation). Universidade Nova de Lisboa.

Matias, D., Joaquim, S., Ramos, M., Sobral, P., Leitão, A., 2011. Biochemical compounds' dynamics during larval development of the carpet-shell clam Ruditapes decussatus (Linnaeus, 1758): effects of mono-specific diets and starvation. Helgol. Mar. Res. 65 (3), 369–379. http://dx.doi.org/10.1007/s10152-010-0230-3.

Maynou, F., Galimany, E., Ramón, M., Solé, M., 2020. Impact of temperature increase and acidification on growth and the reproductive potential of the clam Ruditapes philippinarum using DEB. Estuar. Coast. Shelf Sci. 247, 107099. http://dx.doi.org/10.1016/j.ecss.2020.107099.

Mohammad, S., Belal, A., Hassan, S., 2014. Growth, age and reproduction of the commercially clams Venerupis aurea and Ruditapes decussatus in Timsah Lake, Suez Canal, Egypt. Indian J. Geo-Mar. Sci. 43, 589–600.

Montes, J., Ferro-Soto, B., Conchas, R.F., Guerra, A., 2003. Determining culture strategies in populations of the European flat oyster, Ostrea edulis, affected by bonamiosis. Aquaculture 220 (1), 175–182. http://dx.doi.org/10.1016/S0044-8486(02)00628-2.

Newell, R.I.E., Bayne, B.L., 1980. Seasonal changes in the physiology, reproductive condition and carbohydrate content of the cockle Cardium (=Cerastoderma) edule (Bivalvia: Cardiidae). Mar. Biol. 56 (1), 11–19. http://dx.doi.org/10.1007/BF00390589.

Ojea, J., Pazos, A.J., Martínez, D., Novoa, S., Sánchez, J.L., Abad, M., 2004. Seasonal variation in weight and biochemical composition of the tissues of Ruditapes decussatus in relation to the gametogenic cycle. Aquaculture 238 (1), 451–468. http://dx.doi.org/10.1016/j.aquaculture.2004.05.022.

Pérez-Camacho, A., 1980. Biología de Venerupis pullastra (Montagu) y Venerupis decussata (Linnaeus) (Mollusca, Bivalvia), con especial referencia a los factores determinantes de la producción.

Pérez-Camacho, A., Beiras, R., Albentosa, M., 1994. Effects of algal food concentration and body size on the ingestion rates of Ruditapes decussatus (Bivalvia) veliger larvae. Mar. Ecol. Prog. Ser. 115 (1/2), 87–92, http://www.jstor.org/stable/24849733.

Pérez-Morales, A., A., M.-L., Camalich, J., 2015. Dry weight, carbon, C/N ratio, hydrogen, and chlorophyll variation during exponential growth of selected microalgae species used in aquaculture. CICIMAR Oceán. 30, 33–43. http://dx.doi.org/10.37543/oceanides.v30i1.168.

Pick, J.L., Nakagawa, S., Noble, D.W.A., 2019. Reproducible, flexible and high-throughput data extraction from primary literature: The metaDigitise r package. Methods Ecol. Evol. 10 (3), 426–431. http://dx.doi.org/10.1111/2041-210X.13118.

Prieto, D., Urrutxurtu, I., Navarro, E., Urrutia, M.B., Ibarrola, I., 2018. Mytilus galloprovincialis fast growing phenotypes under different restrictive feeding conditions: Fast feeders and energy savers. Mar. Environ. Res. 140, 114–125. http://dx.doi.org/10.1016/j.marenvres.2018.05.007.

Prins, T.C., Smaal, A.C., Pouwer, A.J., 1991. Selective ingestion of phytoplankton by the bivalvesMytilus edulis L. andCerastoderma edule (L.). Hydrobiol. Bull. 25 (1), 93–100. http://dx.doi.org/10.1007/BF02259595.

Pronker, A.E., Peene, F., Donner, S., Wijnhoven, S., Geijsen, P., Bossier, P., Nevejan, N.M., 2015. Hatchery cultivation of the common cockle (Cerastoderma edule L.): from conditioning to grow-out. Aquacult. Res. 46 (2), 302–312. http://dx.doi.org/10.1111/are.12178.

R Core Team, 2023. R: A language and environment for statistical computing. https://www.R-project.org/.

Rodríguez-Moscoso, E., Arnaiz, R., 1998. Gametogenesis and energy storage in a population of the grooved carpet-shell clam, Tapes decussatus (Linné, 1787), in northwest Spain. Aquaculture 162 (1), 125–139. http://dx.doi.org/10.1016/S0044-8486(98)00170-7.

Rosland, R., Strand, Ø., Alunno-Bruscia, M., Bacher, C., Strohmeier, T., 2009. Applying Dynamic Energy Budget (DEB) theory to simulate growth and bio-energetics of blue mussels under low seston conditions. J. Sea Res. 62 (2), 49–61. http://dx.doi.org/10.1016/j.seares.2009.02.007.

Sarà, G., Reid, G.K., Rinaldi, A., Palmeri, V., Troell, M., Kooijman, S., 2012. Growth and reproductive simulation of candidate shellfish species at fish cages in the Southern Mediterranean: Dynamic Energy Budget (DEB) modelling for integrated multi-trophic aquaculture. Aquaculture 324–325, 259–266. http://dx.doi.org/10.1016/j.aquaculture.2011.10.042.

Serdar, S., Lök, A., 2009. Gametogenic cycle and biochemical composition of the transplanted carpet shell clam Tapes decussatus, Linnaeus 1758 in Sufa (Homa) Lagoon, Izmir, Turkey. Aquaculture 293 (1), 81–88. http://dx.doi.org/10.1016/j.aquaculture.2009.03.052.

Stechele, B., Maar, M., Wijsman, J., Van Der Zande, D., Degraer, S., Bossier, P., Nevejan, N., Cooke, S., 2022. Comparing life history traits and tolerance to changing environments of two oyster species (Ostrea edulis and Crassostrea gigas) through Dynamic Energy Budget theory. Conserv. Physiol. 10 (1), coac034. http://dx.doi.org/10.1093/conphys/coac034.

Steeves, L.E., 2022. Feeding Physiology of Suspension-Feeding Bivalves: Inter- and Intraspecific Plasticity (Doctoral dissertation). Dalhousie University, Halifax, Nova Scotia.

Taylor, D., Larsen, J., Buer, A.-L., Friedland, R., Holbach, A., Petersen, J.K., Nielsen, P., Ritzenhofen, L., Saurel, C., Maar, M., 2021. Mechanisms influencing particle depletion in and around mussel farms in different environments. Ecol. Indic. 122, 107304. http://dx.doi.org/10.1016/j.ecolind.2020.107304.

The MathWorks Inc., 2023. MATLAB (R2023b). https://www.mathworks.com.

Tyler-Walter, H., 2007. Common cockle (Cerastoderma edule). https://www.marlin.ac.uk/species/detail/1384.

Urrutia, M.B., Ibarrola, I., Iglesias, J.I.P., Navarro, E., 1999. Energetics of growth and reproduction in a high-tidal population of the clam Ruditapes decussatus from Urdaibai Estuary (Basque Country, N. Spain). J. Sea Res. 42 (1), 35–48. http://dx.doi.org/10.1016/S1385-1101(99)00017-9.

van der Meer, J., 2006. An introduction to Dynamic Energy Budget (DEB) models with special emphasis on parameter estimation. J. Sea Res. 56 (2), 85–102. http://dx.doi.org/10.1016/j.seares.2006.03.001.

van der Meer, J., 2020. Limits to food production from the sea. Nat. Food 1 (12), 762–764. http://dx.doi.org/10.1038/s43016-020-00202-8.

van der Meer, J., Hin, V., van Oort, P., van de Wolfshaar, K.E., 2022. A simple DEB-based ecosystem model. Conserv. Physiol. 10 (1), coac057. http://dx.doi.org/10.1093/conphys/coac057.

van der Meer, J., Tjui Yeuw, T., de Wolfshaar, v., Can trophic efficiency differences among 1 populations be explained by physiology?. Tech. rep., (n.d.).

van der Veer, H.W., Cardoso, J.F.M.F., van der Meer, J., 2006. The estimation of DEB parameters for various Northeast Atlantic bivalve species. J. Sea Res. 56 (2), 107–124. http://dx.doi.org/10.1016/j.seares.2006.03.005.

van Riel, A.-J., Nederlof, M.A.J., Chary, K., Wiegertjes, G.F., de Boer, I.J.M., 2023. Feed-food competition in global aquaculture: Current trends and prospects. Rev. Aquaculture 15 (3), 1142–1158. http://dx.doi.org/10.1111/raq.12804.

van Stralen, M.R., Dijkema, R.D., 1994. Mussel culture in a changing environment: the effects of a coastal engineering project on mussel culture (Mytilus edulis L.) in the Oosterschelde estuary (SW Netherlands). Hydrobiologia 282 (1), 359–379. http://dx.doi.org/10.1007/BF00024642.

Whyte, J.N.C., Englar, J.R., Carswell, B.L., 1990. Biochemical composition and energy reserves in Crassostrea gigas exposed to different levels of nutrition. Aquaculture 90 (2), 157–172. http://dx.doi.org/10.1016/0044-8486(90)90338-N.

Wijsman, J.W.M., Troost, K., Fang, J., Roncarati, A., 2019. Global production of marine bivalves. Trends and challenges. In: Smaal, A.C., Ferreira, J.G., Grant, J., Petersen, J.K., Strand, Ø. (Eds.), Goods and Services of Marine Bivalves. Springer International Publishing, Cham, pp. 7–26. http://dx.doi.org/10.1007/978-3-319-96776-9{_}2.